Investigations of Processing Methods for GaN-Based Laser Diodes

Mohamed Fikry

The development of an optimized recipe for the processing of a MQW AlGaInN based oxide stripe laser diode grown on c-plane sapphire has been investigated. Two processing sequences involving Reactive Ion Etching (RIE) were compared. The first relied on the use of SiO_2 *as a dry etch-mask, whereas in the second, the use of nickel was utilized. The critical step of smooth and vertical mirror formation played a significant role in dictating the choice of the dry-etch mask material. A facet inclination angle of 80° was achieved. Under pulsed electrical current injection, we measured a threshold current density of 6.1 kA/cm*^{2} *on the laser device.*

1. Introduction

Lately, laser diodes based on the group-III nitirde material system have been receiving a large attention along with the rapid emerge of short wavelength optoelectronics. They can be considered as promising candidates for a wide variety of applications including high density information storage on optical media, projection displays in addition to possible treatments in the medical field [1].

One critical parameter that can greatly influence the performance of the lasing device is the facet or mirror quality of the resonator, which can directly influence the percentage of optical feedback. The smoothness and degree of anisotropy of the facet can thus play a significant role. For III-nitrides grown on c-plane sapphire substrates, mirror formation by cleavage gets very difficult due to a 30 ° rotation of the GaN layer with respect to the sapphire wafer [2]. Furthermore, due to the high chemical stability of the nitrides, the use of wet etching techniques becomes more challenging.

A number of dry etching techniques can be applied for the afore-mentioned material system including Reactive-Ion-Etching (RIE), Chemically Assissted Ion Beam Etching (CAIBE) as well as Inductively Coupled Plasma (ICP). The choice of the mask material in the dry etch process (selectivity between mask material and material to be etched), along with the etching conditions inside the reactor (pressure, power and the choice of gases), can significantly influence the final etched facet profile [3]. In addition, there exists a very high degree of sensitivity to any minor alterations to the lithography conditions that would dictate the pattern to be transferred to the etched feature.

In this work, we present a comparison of two processing sequences based on RIE using two different mask materials (SiO_2 and nickel) for an MOCVD grown laser structure on c-plane sapphire substrate. In addition, characterization of the laser device under pulsed current injection is reported.

2. Epitaxial Structure

The MOVPE growth sequence for the investigated samples is shown in a simplified manner in Fig. 1. The detailed growth sequence is described as follows. Starting from a c-plane oriented sapphire substrate, an undoped GaN buffer layer of 1.3 µm involving AlN nucleation and a SiN monolayer for defect reduction is grown [4]. After that, two subsequent layers of silicon doped GaN with doping concentrations of $5 \times 10^{18}\,\mathrm{cm}^{-3}$ and $1 \times 10^{19}\,\mathrm{cm}^{-3}$ and thicknesses of 750 nm and 300 nm are used for providing n-doping and improving the carrier injection at the n-contacts. Then 410 nm of $Al_{0.09}Ga_{0.91}N$:Si together with 100 nm GaN:Si are grown for the optical confinement of the laser mode (Separate Confinement Heterostructure). The multi-quantum well (MQW) active region consists of 2 quantum wells of 2.6 nm $In_{0.09}Ga_{0.91}N$ separated by 12 nm GaN barriers. A spacer layer of 20 nm followed by a highly doped $Al_{0.2}Ga_{0.8}N$: Mg (p-AlGaN) electron barrier layer of 10 nm comes directly above the MQWs. The layer sequence starting from the n-AlGaN to the start of the MQWs is approximately mirrored to the p-side directly above the afore-mentioned carrier confinement layer. The top most two layers are a 60 nm highly doped p-GaN (around $6 \times 10^{19}\,\mathrm{cm}^{-3}$) followed by a 20 nm p-cap doped as high as $1 \times 10^{20}\,\mathrm{cm}^{-3}$ for the formation of a good ohmic contact.

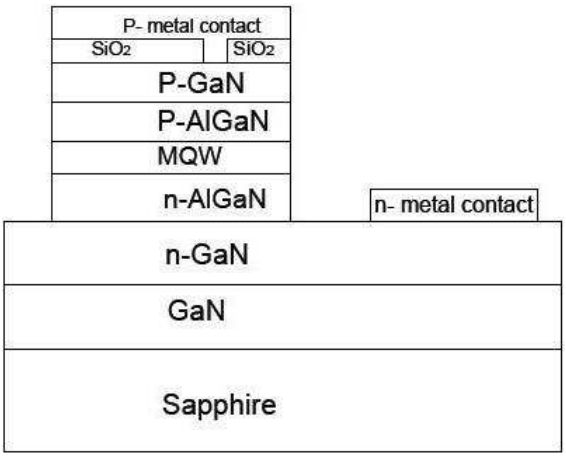

Fig. 1: Epitaxial structure and layout of laser device after processing.

3. Laser Processing Using a SiO_2 Dry-Etch Mask

The process sequence that has been followed as a starting point for the investigations is summarized as follows: (1) Thermal activation of the Mg dopant atoms for generation of holes at 750 °C for 1 minute, (2) PECVD deposition of SiO_2 as a passivation layer, (3) defining the SiO_2 mesa dimensions using photolithography and RIE involving CF_4 plasma, (4) dry etching of the GaN resonator using Cl_2, BCl_3 and Ar plasma RIE, (5) dry etching of the oxide stripe in a CF_4 plasma RIE, and finally, (6) p- and n- contact

formation using electron beam evaporation of the necessary metals and Rapid Thermal Annealing (RTA).

A number of problems have been observed for the use of SiO_2 as a direct dry-etch mask in the Cl_2 based plasma RIE. First, we observed the formation of highly dense micro-pillars (also referred to as surface grass) on the etched n-GaN layer (Fig. 2). These micro-pillars can be removed by a subsequent step of KOH crystallographic wet etching. However, the removed grass leaves a very rough surface morphology (Fig. 3) that is assumed to considerably degrade the contact resistance for the n-contact.

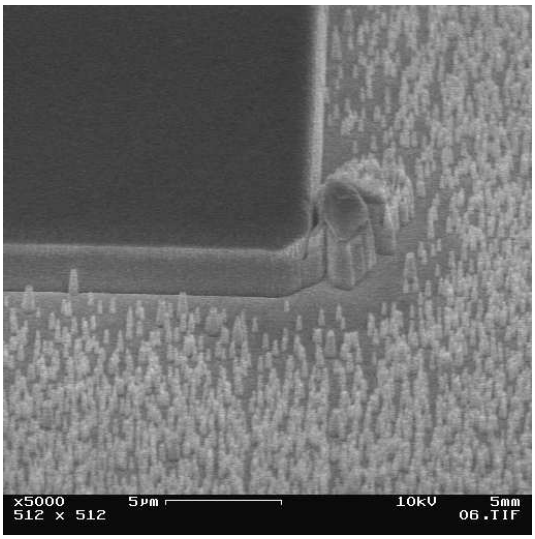

Fig. 2: Dense grass formation after GaN dry etching.

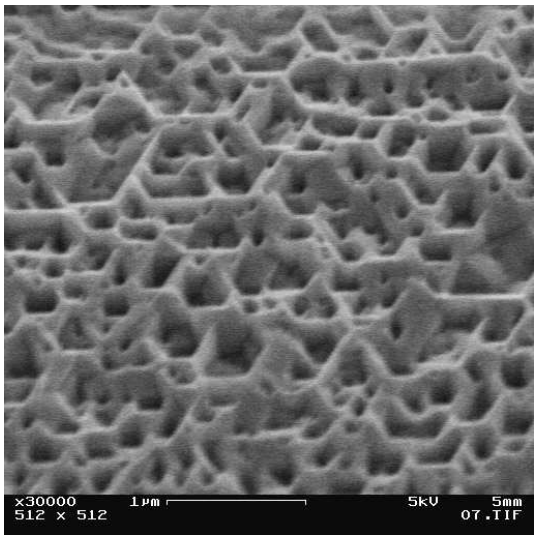

Fig. 3: Rough n-GaN floor after removal of grass pillars using hot KOH solution.

Obviously, small SiO_2 particles sputtered from the mask material as well as from the quartz substrate holder acted as micro-masking particles during dry etching. As the etch rate of SiO_2 is a factor of 6 to 7 less than that of GaN, the GaN directly underneath the micro-SiO_2 particles is not etched, thus revealing a pillar shape [5].

Another problem related to the SiO_2 masking properties was the generation of etched facets with highly rough surfaces (Fig. 4). Such a high degree of facet roughness is expected to degrade the mirror reflectivity needed for lasing action.

Finally, it was also observed that the etched facet exhibited a two-sloped sidewall profile (mask facetting effect). In other words, the upper part of the etched feature exhibit a smaller slope as compared to the lower one (Fig. 5). This phenomenon could be explained as a lateral shrinkage of the mask material as explained in [5] and [3]. The solution to this problem is either to use a higher thickness of the mask material and hence mask facetting would not reach the GaN mesa top edge within the etching time, or to use another mask material that is more resistant to the employed etch conditions. However, using a thicker mask would cause more difficulties for the fore-coming step of stripe opening etching [5].

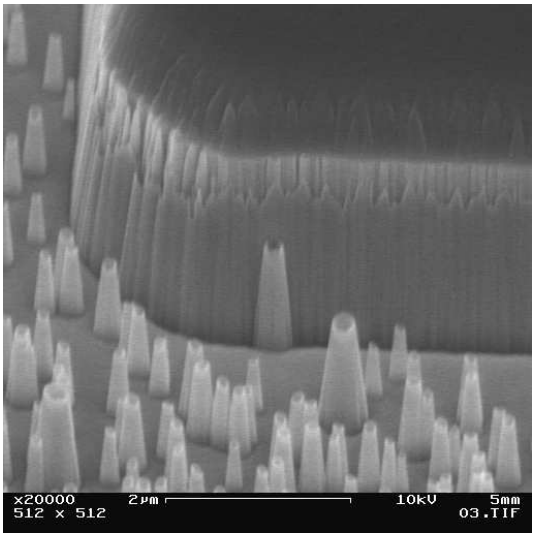

Fig. 4: Rough sidewall surfaces generated using a Sio_2 dry-etch mask.

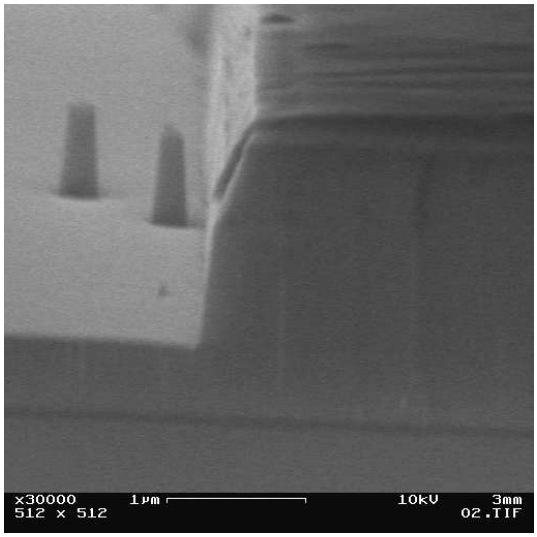

Fig. 5: A two-sloped sidewall profile generated due to mask facetting effect.

4. Optimization of Resonator Formation

As a counter measure for the afore-mentioned problems, investigations for optimization of the dry etching using a different mask material were performed. According to [3] and [6], the resulting sidewall inclination angle is directly influenced by the original mask sidewall profile and the selectivity of the mask material to the etched material. Nickel was chosen as it possesses a higher selectivity to GaN than SiO_2 with the respective values of 18 and 6 [7]. Hence, it is more etch resistant and can generate higher slopes of the etched facet. Additionally, nickel has a lower sputter yield in comparison to amorphous SiO_2 due to the different material structure and chemistry. This reduces the effects of grass as well as mask facetting. Thus the necessary mask thickness during dry etching can be reduced. Finally, process sensitivities during RIE are reduced leading to a higher degree of reproducibility.

First, we investigated a nickel film of 100 nm thickness for an etch time of 20 minutes using a graphite substrate holder (as the formerly used quartz holder proved to contribute to further grass formation [5]). Indeed, now the formation of grass pillars was completely suppressed at the etched n-GaN layer (Fig. 6 left). Additionally, the generated profiles were characterized by relatively smooth facet surfaces (Fig. 6 right).

We thus investigated an alternative mirror processing sequence using nickel as a dry etch mask. Moreover, it should exhibit a lower degree of RIE process sensitivities (such as fluctuations in substrate temperature or reactor pressure) and impose less limitations for other critical steps (such as oxide stripe etching) [5]. The new processing sequence involved the use of a double dry etch mask of nickel on top of sputter deposited SiO_2. The latter was deposited in a structured manner allowing for an already open oxide stripe (thus eliminating the need for an extra processing step). The generated laser facets were characterized by an average angle of 79 to 80 ° (Fig. 7 left). Nevertheless, laser action was achieved. A detailed description for the steps of our new suggested processing sequence

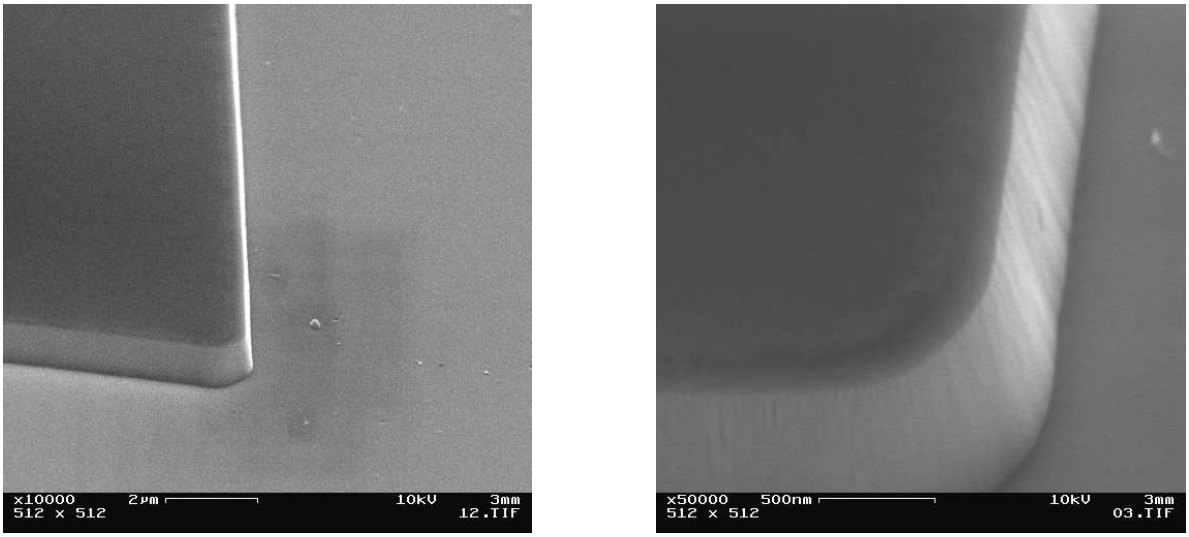

Fig. 6: Clean n-GaN surfaces (left) and smooth etched sidewalls (right) after the use of nickel as a mask material with a graphite plate.

can be found in [5].

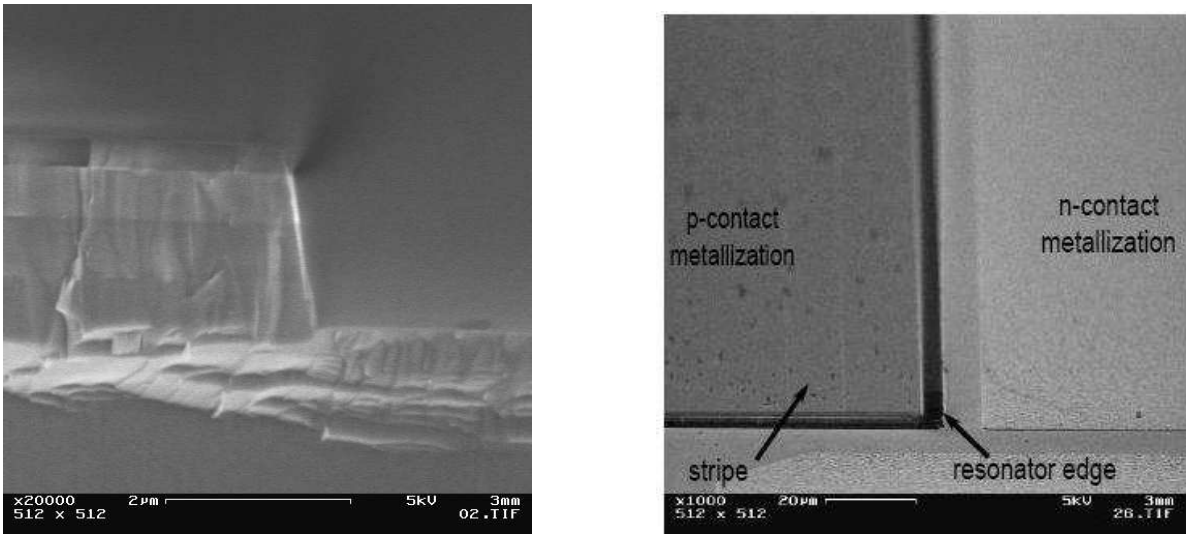

Fig. 7: Sidewall inclination of the resonator edges (angle 79-80 °) (left). SEM image of a complete fabricated device (right).

Contact formation for the n-contact was achieved for a metal stack of Ti/Al/Ni/Au with thicknesses of 15, 220, 40 and 50 nm, respectively, annealed in a nitrogen environment at 500 °C for 5 minutes. The resulting contact resistivity (ρ_c) was evaluated to be $9 \times 10^{-6}\,\Omega\text{cm}^2$ using the Circular Transmission Line Method model for contact characterization [8]. P-contact optimization was achieved using a metallization scheme involving a 20 nm palladium layer followed by a 100 nm gold layer, where the optimized alloying parameters are the same as for the n-contact. The resulting p-contact resistivity was calculated to be $1 \times 10^{-3}\,\Omega\text{cm}^2$. Furthermore, an additional gold cap layer of 800 nm

was evaporated after annealing for better current conduction. A SEM picture of a fully processed device is depicted in Fig. 7 (right).

5. Characterization

Measurements involving current-voltage (I-V) and power-current (P-I) characteristics for the laser device were undergone using pulsed current injection at a pulse width of 100 ns (Fig. 8). We measured a threshold current density of 6.1 kA/cm^2 and a voltage at threshold of 10 V. Measurements took place on wafer, where no direct non-obstructed light paths from the facet to the detector existed. Moreover, the aforementioned characterization values where recorded without any mirror coatings. Spectral analysis under stimulated emission revealed a peak wavelength of 393 nm (Fig. 9).

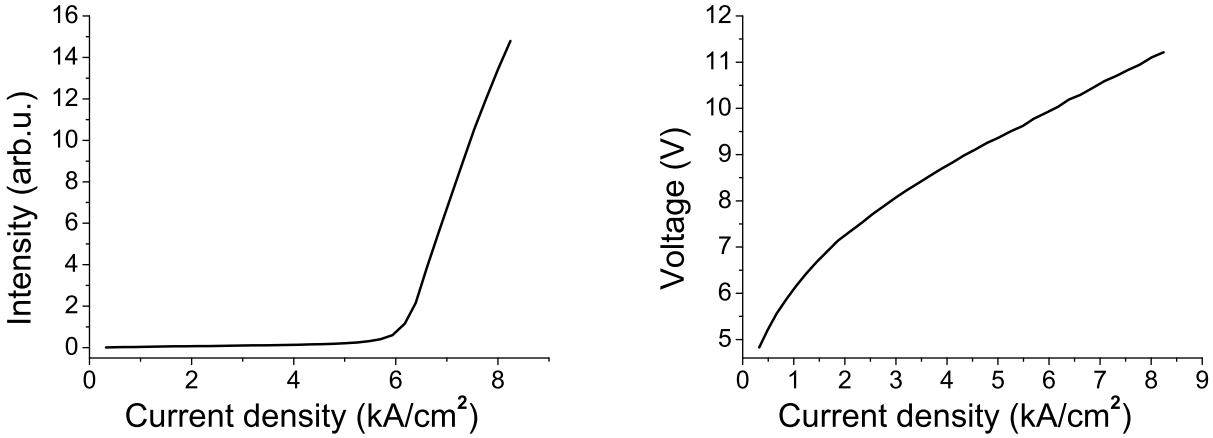

Fig. 8: Scaled optical power (per facet) vs current density (Left). Measured voltage-current characteristics for the laser device (Right). Stripe length: 800 µm. Stripe width: 12 µm. Pulse frequency: 10 kHz.

6. Conclusion

A number of problems characterizing the use of SiO_2 as dry etch mask for mirror formation in a GaN based oxide stripe laser diode have been studied. The use of nickel has proven to eliminate appearance of grass pillars and to reveal smooth etched feature. The final sidewall angle of 79 to 80 ° revealed a threshold current density of 6.1 kA/cm^2 under pulsed operation.

7. Acknowledgments

We would gratefully acknowledge the cooperation of M.Sc. H.C. Xu for his introductory training with the fabrication tools and his previous work on the same topic, Dipl.-Ing. W. Schwarz for his help with sputter coating, Mr. R. Rösch for his help with RIE and Ms. S. Menzel for her help with experiments involving wet etching.

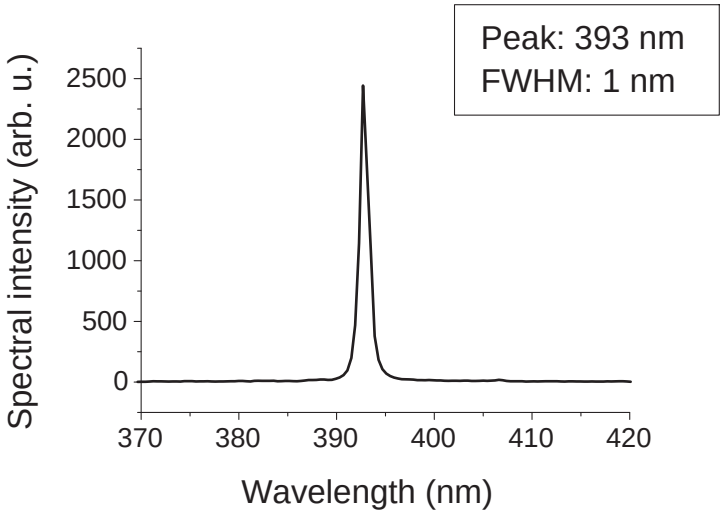

Fig. 9: Spectral analysis under stimulated emission for the laser device.

References

[1] S. Nakamura. "Laser Diodes", *Optoelectronic properties of semiconductors and superlattices*, Vol. 7, *GaN and Related Materials II*, Stephan J. Pearton (Ed.) pp. 1–44, 2000.

[2] H.Z. Xiao, N.E. Lee, R.C. Powell, Z. Ma, L.J. Chou, L.H. Allen, J.E. Greene and A. Rockett, "Defect ordering in epitaxial α-GaN(0001)" *J. Appl. Phys.* vol. 76, no. 12, 1994.

[3] M.J. Madou. *Fundamentals of Microfabrication: The Science of Miniaturization*, (2nd ed.), 2002.

[4] J. Hertkorn, P. Brueckner, S.B. Thapa, T. Wunderer, F. Scholz, M. Feneberg, K. Thonke, R. Sauer, M. Beer and J. Zweck. "Optimzation of nucleation and buffer layer growth for improved GaN quality", *J. Crystal Growth*, vol. 308, pp. 30–36, 2007.

[5] M. Fikry, *Epitaxy and processing of AlGaInN heterostructures for light emitting diode applications*. Master thesis, Institute of Optoelectronics, University of Ulm, August 2008.

[6] H.C. Xu. *Investigations of RIE processing for the controlled characterization of optoelectronic properties of nitride based devices*. Master thesis, Institute of Optoelectronics, University of Ulm, August 2007.

[7] M. Dineen. Oxford Instruments Ltd. Private communication, 2007.

[8] A. Weimar, A. Lell, G. Bruederl, S. Bader and V. Haerle. "Investigations of Low-Resistance Metal Contacts on p-Type GaN using the Linear and Circular Transmission Line Method", *phys. stat. sol. (a)* vol. 183, no. 169, 2001.